JOURNAL OF VIROLOGY, Dec. 2007, p. 12899–12910 Vol. 81, No. 23
0022-538X/07/$08.00+0 doi:10.1128/JVI.01280-07

Myristoylation Is Required for Human Immunodeficiency Virus Type 1 Gag-Gag Multimerization in Mammalian Cells[▽]

Hua Li,† Jun Dou, Lingmei Ding, and Paul Spearman*

Departments of Pediatrics and Microbiology and Immunology, Emory University, Atlanta, Georgia 30322

Received 12 June 2007/Accepted 7 September 2007

The Gag protein of human immunodeficiency virus type 1 directs the virion assembly process. Gag proteins must extensively multimerize during the formation of the spherical immature virion shell. In vitro, virus-like particles can be generated from Gag proteins that lack the N-terminal myristic acid modification or the nucleocapsid (NC) protein. The precise requirements for Gag-Gag multimerization under conditions present in mammalian cells, however, have not been fully elucidated. In this study, a Gag-Gag multimerization assay measuring fluorescence resonance energy transfer was employed to define the Gag domains that are essential for homomultimerization. Three essential components were identified: protein-protein interactions contributed by residues within both the N- and C-terminal domains of capsid (CA), basic residues in NC, and the presence of myristic acid. The requirement of myristic acid for multimerization was reproduced using the heterologous myristoylation sequence from v-*src*. Only when a leucine zipper dimerization motif was placed in the position of NC was a nonmyristoylated Gag protein able to multimerize. These results support a three-component model for Gag-Gag multimerization that includes membrane interactions mediated by the myristoylated N terminus of Gag, protein-protein interactions between CA domains, and NC-RNA interactions.

Human immunodeficiency virus type 1 (HIV-1) particles assemble on cellular membranes. $Pr55^{Gag}$ (Gag) is a precursor polyprotein that drives the assembly process and forms the shell of the developing particle. Gag molecules first form an electron-dense plaque underlying the plasma membrane to which additional Gag molecules are added as the developing particle bud enlarges and generates increasing membrane curvature. A spherical particle with an immature core is generated, which is released from the membrane through late budding events involving the cellular ESCRT machinery. $Pr55^{Gag}$ is cleaved by the viral protease during the budding process, triggering structural shifts that generate the mature conical core of the virus. Gag cleavage products, from the N to C terminus, include matrix (MA), capsid (CA), spacer peptide 1 (SP1), nucleocapsid (NC), spacer peptide 2 (SP2), and p6.

Gag-Gag multimerization is essential to the process of retrovirus budding and particle formation. CA plays a central role in mediating Gag-Gag interactions (15, 17, 24, 26, 41, 42). CA-CA contacts in the mature conical core have been defined using X-ray crystallographic analysis of purified CA protein and cryoelectron microscopic reconstructions of assembled CA-CA cylinders and cores (5, 15–17, 26). CA consists of two distinct domains, an N-terminal domain (NTD) and a C-terminal domain (CTD), separated by a short flexible linker. The CA CTD includes a dimer interface that is created by the parallel packing of helix 9 of two CTDs (15). The mature core has been modeled as a lattice in which six CA molecules form a hexagonal ring through interactions of their NTDs, while the CTD dimer interface connects with surrounding hexamers (26). Mutation of key residues within the CTD dimer interface disrupts dimer formation and eliminates particle infectivity but also greatly reduces the assembly of retroviral particles, suggesting that dimer interface contacts are important not just in the mature core but also in the developing immature particle (15). NTD-NTD interactions may also be formed during assembly and prior to maturation, as mutations of key residues involved in NTD interactions also disrupt particle formation (41). The importance of NTD-NTD interactions was supported by a hydrogen-deuterium exchange study in which peptides representing CA helices I and II were protected from proteolytic digestion in both mature and immature virus-like particles (25). Taken together, it is likely that both NTD-NTD and CTD-CTD (dimer interface) contacts are important during the assembly process.

In addition to CA, NC plays a critical role in Gag-Gag multimerization. Mapping by yeast two-hybrid analysis initially identified the minimal site of multimerization of Gag as that sequence between the C-terminal one-third of CA and the C terminus of NC (14). Replacement of the entire NC domain of Gag with a leucine zipper (LZ) dimerization motif rescues particle formation, providing strong indirect evidence that NC contributes to Gag-Gag multimerization (43). The ability of NC to promote Gag-Gag interactions may be attributable to its ability to bind RNA. In support of this model, RNA promoted the assembly of spherical particles from Rous sarcoma virus CA-NC protein (9) and from a recombinant HIV Gag protein lacking the p6 region (8). Substitution of a short DNA oligonucleotide for RNA allowed the dimerization of Rous sarcoma virus Gag, supporting a model in which Gag-RNA interactions promote Gag-Gag dimerization followed by the formation of larger oligomers (28). Sequences within NC contribute to the density of retroviral particles, suggesting an important role for an RNA bridge during Gag-Gag multimerization (35, 36). This function of NC has been termed the "I," or interaction, do-

* Corresponding author. Mailing address: Pediatric Infectious Diseases, Emory University, 2015 Uppergate Drive, Atlanta, GA 30322. Phone: (404) 727-5642. Fax: (404) 727-9223. E-mail: paul.spearman@emory.edu.

† Present address: Wistar Institute, Philadelphia, PA 19104.

▽ Published ahead of print on 19 September 2007.

main. Using a fluorescence resonance energy transfer (FRET)-based assay of living cells, we previously demonstrated that Gag-Gag FRET requires the contribution of the "I" domain function of NC (12).

In contrast to the abundant literature supporting a role for CA and NC in mediating Gag-Gag interactions, there has been relatively little published evidence indicating that Gag-membrane interactions promote multimerization. Myristoylation of Gag on its N-terminal glycine residue is essential for particle formation (6, 19). Myristoylated Gag is membrane associated, while nonmyristoylated Gag is "loosely" membrane associated, as indicated by membrane fractionation studies (13, 38, 44). Myristate confers increased binding affinity upon the MA protein, as measured using model membrane systems, although the binding of MA is also dependent upon ionic interactions between basic residues and negatively charged phospholipids (11, 44). The interaction of the N terminus of Gag with membranes is facilitated by a myristoyl switch (31, 37, 45). Myristate occupies a shallow cavity within the globular head of MA and can be triggered to become more accessible to membranes upon multimerization (39). The myristoyl switch can also be triggered by interactions with phosphatidylinositol 4,5-bisphosphate (33), an interaction that could help to explain the selective interaction of Gag with the cytosolic face of the plasma membrane during assembly.

Here, we report an additional role for myristic acid in the assembly process. We used a FRET-based assay to assess Gag-Gag interactions in living cells and introduced a series of mutations designed to disrupt CA-CA interactions, NC-RNA interactions, and the myristoylation of HIV Gag. Myristic acid was found to be essential for Gag-Gag interaction in living cells. Gag-Gag FRET was seen in membrane and not cytosolic fractions, suggesting that the primary contribution of myristate to multimerization lies in its influence on membrane interaction. Gag-Gag FRET was eliminated by specific targeted mutations within CA and NC in a Gag protein that maintained an intact myristoylation site. Together, these data support a model in which three components are essential to achieve Gag-Gag multimerization: NC-RNA interactions, CA-CA interactions, and interaction of the myristoylated N terminus of Gag with cellular membranes.

MATERIALS AND METHODS

Plasmid construction. The *gag* coding sequences for all expression constructs in this study were derived from the codon-optimized version of HXB2 Gag as previously described (12). Gag proteins were cloned as fusion constructs with the cerulean variant of cyan fluorescent protein (CFP) (32) or the Venus variant of yellow fluorescent protein (YFP) (30). CFP and YFP fusions were expressed in plasmids pcDNA4/TO and pcDNA5/TO (Invitrogen), respectively, except for CFP alone and Src-CFP, which were constructed in vector pECFP-C1, and YFP and Src-YFP were in the pEYFP-N3 vector (BD Clontech). CFP and YFP expression constructs were generated by first PCR amplifying cerulean or Venus coding regions into the BamHI and NotI sites in pcDNA4/TO and pcDNA5/TO and then placing the Gag reading frame in the plasmid using a HindIII site at the 5′ end and a BamHI site at the 3′ end. The LZ sequence was a kind gift from Chen Liang (20) and was placed in frame into the indicated constructs using PCR cloning. Some individual nucleotide substitutions were introduced using the QuikChange II site-directed mutagenesis kit (Stratagene), including SrcCA(W184A+M185A)NC-cerulean/Venus, Myr(−)SrcCA(W184A+M185A)NC-cerulean/Venus, SrcCA(M39A+W184A+M185A)NC-cerulean/Venus, Myr(−)SrcCA(M39A+W184A+M185A)NC-cerulean/Venus, SrcCA(M39A+W184A+M185A)NC15A-cerulean/Venus, and Myr(−)SrcCA(M39A+W184A+M185A)NC15A-cerulean/Venus.

A schematic diagram of the Gag-cerulean and Gag-Venus expression constructs employed in this study is shown in Fig. 1. Oligonucleotide primers used for all PCR amplifications used to generate the panel of constructs in Fig. 1 are available upon request.

Cells and transfections. 293T and HeLa cells were maintained in Dulbecco's modified Eagle medium with 10% fetal bovine serum with penicillin and streptomycin at 37°C in 5% CO_2. 293T cells were grown in 10-cm tissue culture dishes. Transfections of all fusion constructs into 293T cells were performed by the calcium phosphate transfection method using 5 to 10 μg of total plasmid DNA. For fluorescence microscopy analysis, HeLa cells were grown in six-well plates with the microscopy glass coverslips (tissue culture treated; Fisher Scientific) and transfected with Lipofectamine 2000 (Invitrogen) using a total of 2 ug of plasmid DNA.

Isolation of cytosolic and membrane fractions. Cells were harvested for analysis 36 h posttransfection. One 10-cm^2 tissue culture dish of nearly confluent 293T cells was used in each experimental sample. Cells were washed in NTE buffer (100 mM NaCl, 10 mM Tris-Cl [pH 8.0], 1 mM EDTA [pH 8.0]) and then allowed to swell in hypotonic buffer (10 mM Tris-Cl [pH 8.0], 1 mM EDTA [pH 8.0]) plus protease inhibitors for 20 min on ice. Cells were then broken by Dounce homogenization. After the buffer was adjusted to 0.1 M NaCl, the nuclei and unbroken cells were removed by centrifugation at 1,000 × *g* for 10 min. The supernatants containing cytosolic and membrane components were then adjusted to 50% iodixanol from a stock solution of 60% iodixanol (Nycomed Pharma, Oslo, Norway), and 40% and 10% solutions of iodixanol were then layered on top of the 50% iodixanol layer. The preparation was then centrifuged in a Beckman SW41 rotor at 35,000 rpm for 16 h at 4°C, after which fractions were harvested from the top of the gradient and then analyzed directly by cuvette fluorometry.

Scanning cuvette fluorometry for FRET. Cells cotransfected with Gag-CFP and Gag-YFP constructs were analyzed at 36 h posttransfection. Cells were washed with phosphate-buffered saline (PBS) three times and then harvested directly in PBS for analysis by scanning fluorometry. Selected samples were lysed in lysis buffer (PBS plus 1% NP-40) plus protease inhibitors for comparison with intact cells. Cells and gradient fractions involved in this study were analyzed by fluorometry in a PTI T-format scanning cuvette spectrofluorometer (Photon Technology International, Lawrenceville, NJ). For FRET analysis, samples were excited at 433 nm, and an emission scan ranging from 460 nm to 550 nm was obtained. For the analysis of relative YFP expression, samples were excited at 514 nm, with a resulting emission scan of 524 nm to 550 nm. Samples were also excited at 433 nm, with a resulting emission scan of 460 nm to 480 nm, for analysis of CFP emission in order to compare their CFP expression levels. Data were collected from at least three independent experiments for each construct, and the curves shown are representative of the three measures obtained.

Laser confocal fluorescence microscopy. HeLa cells were grown on glass coverslips and transfected with Gag-CFP or Gag-YFP expression constructs. Cells were washed and fixed after 24 h posttransfection with 40% paraformaldehyde solution (Electron Microscopy Sciences) for 10 min. Images were obtained using a Zeiss LSM 510 laser scanning confocal microscope (Carl Zeiss Inc., Thornwood, NY).

Western blotting to confirm expression of all fusion constructs. Transfected 293T cells were harvested 36 h posttransfection. Cells were lysed in radioimmunoprecipitation assay buffer (25 mM Tris-HCl [pH 7.6], 150 mM NaCl, 1% NP-40, 1% sodium deoxycholate, 0.1% sodium dodecyl sulfate) and examined by Western blotting using anti-green fluorescent protein rabbit serum (Invitrogen) as the primary antibody and goat anti-rabbit (IRDye800; Li-Cor Biosciences) as the secondary antibody. Blots were imaged using infrared fluorescence detection (Li-Cor Odyssey).

RESULTS

Myristoylation of Gag is required for Gag-CFP/Gag-YFP FRET. Gag-CFP/Gag-YFP FRET can detect Gag-Gag interactions in living cells. We previously employed this technique to better define the role of NC in Gag-Gag interactions and demonstrated that Gag-Gag FRET can be detected microscopically on the plasma membrane and on intracellular membranes. It was surprising to us that Gag-Gag FRET was found only in membrane fractions and could not be detected in the cytosol (12), suggesting that the membrane interaction was essential. The present study was designed to further define the requirements for Gag-Gag interactions in living cells by ex-

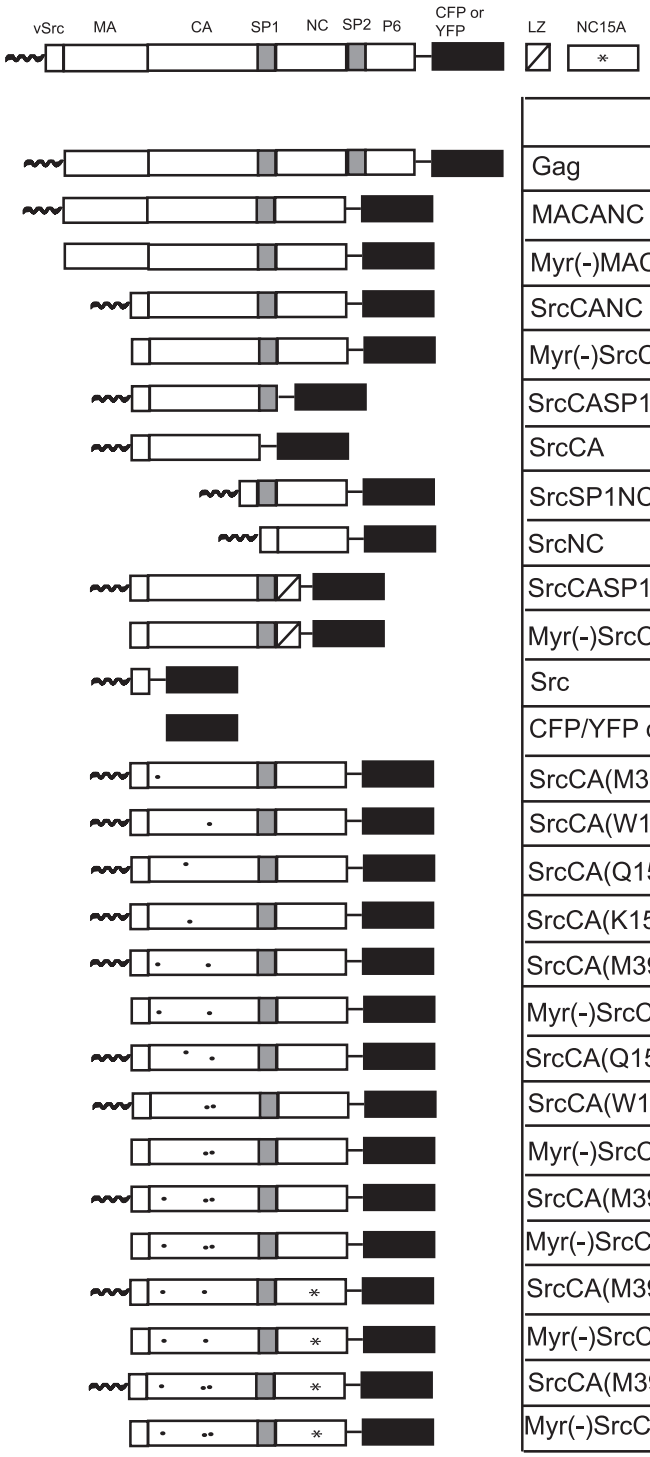

Gag Construct	FRET	Intermediate FRET	NO FRET
Gag	+		
MACANC	+		
Myr(-)MACANC			+
SrcCANC	+		
Myr(-)SrcCANC			+
SrcCASP1		+/-	
SrcCA		+/-	
SrcSP1NC		+	
SrcNC		+	
SrcCASP1LZ(Leucine Zipper)	+		
Myr(-)SrcCASP1LZ(Leucine Zipper)	+		
Src		+/-	
CFP/YFP only			+
SrcCA(M39A)NC		+	
SrcCA(W184A)NC		+	
SrcCA(Q155N)NC		+	
SrcCA(K158A)NC		+	
SrcCA(M39A+W184A)NC		+	
Myr(-)SrcCA(M39A+W184A)NC			+
SrcCA(Q155N+W184A)NC		+	
SrcCA(W184A+M185A)NC		+	
Myr(-)SrcCA(W184A+M185A)NC			+
SrcCA(M39A+W184A+M185A)NC		+	
Myr(-)SrcCA(M39A+W184A+M185A)NC			+
SrcCA(M39A+W184A)NC15A		+	
Myr(-)SrcCA(M39A+W184A)NC15A			+
SrcCA(M39A+W184A+M185A)NC15A			+
Myr(-)SrcCA(M39A+W184A+M185A)NC15A			+

FIG. 1. Schematic representation of Gag-CFP and Gag-YFP constructs described in this study. On the left is a schematic corresponding to the domains pictured in full-length Gag at the top of the diagram. The dark wavy line at the N terminus of pictured proteins represents myristic acid. Dots in CA represent NTD or CTD alanine substitutions; asterisks in NC represent NC15A. The table at the right summarizes results of scanning fluorometry, described as strong FRET (left column), intermediate FRET or, in some cases, slightly detectable FRET (+/−) (middle column), or no FRET detected (right column).

panding on the live-cell FRET assay. We therefore generated a panel of Gag and control fusion proteins, as depicted in Fig. 1. Each of these constructs was cloned as a CFP and as a YFP fusion using enhanced versions of CFP (cerulean) and YFP (Venus) to optimize the performance of CFP-YFP FRET. The panel was designed to test the role of myristic acid, of CA-CA contacts in the NTD (M39A) (41), of CA-CA contacts in the dimer interface of the CA CTD (W184A and M185A) (15),

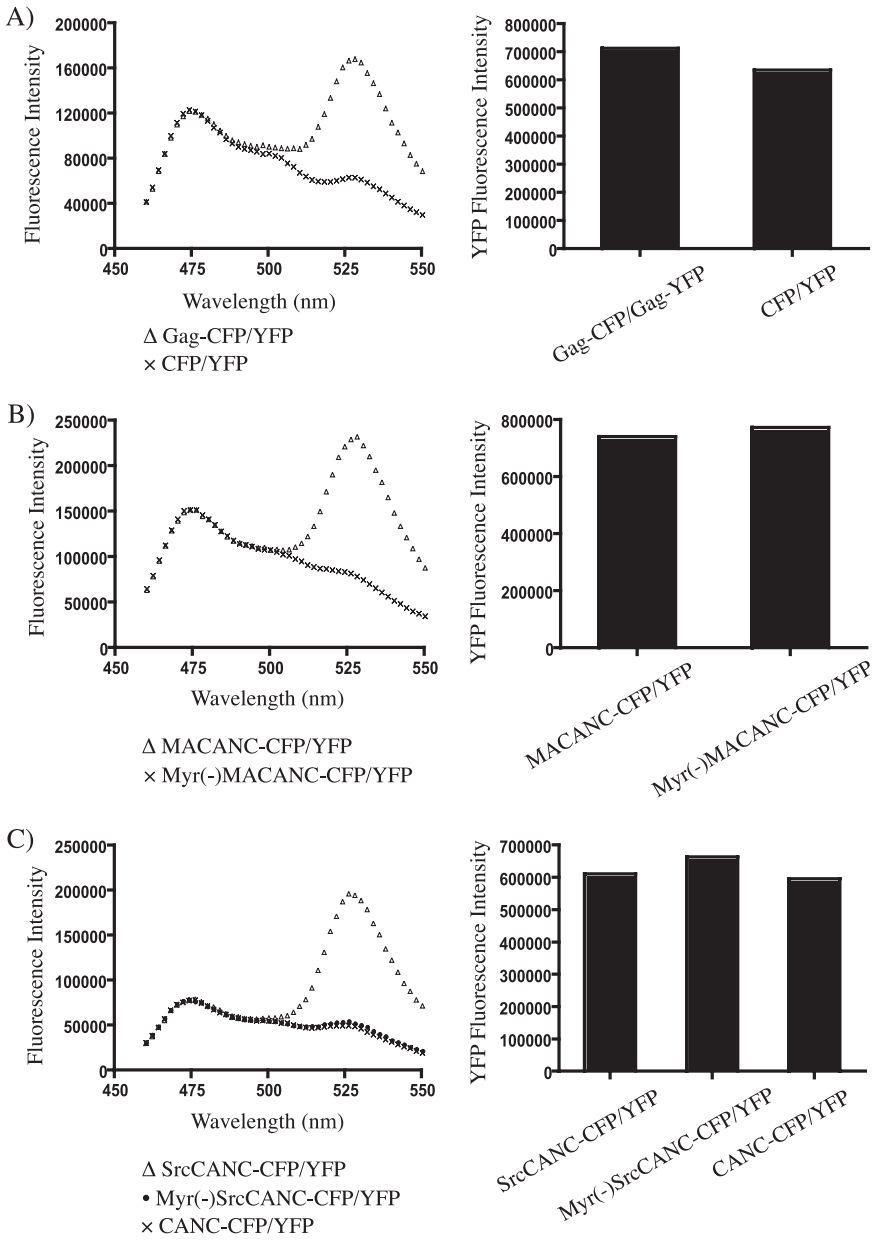

FIG. 2. Requirement of myristoylation for Gag-Gag FRET. Pictured are emission scans of cell suspensions following excitation at 433 nm; the peak at 527 nm represents CFP/YFP FRET. Bars to the right demonstrate that YFP acceptor concentrations were approximately equal for each comparison. The legend for the symbols is provided below each panel.

and of basic residues in NC in contributing to Gag-Gag interactions. In addition, specific mutations in the major homology region (MHR) predicted to disrupt the formation of a proposed domain-swapped dimer based on the zinc finger-associated SCAN domain (Q155N and K158A) (22) were tested.

Gag-Gag FRET was measured in cells expressing paired CFP and YFP constructs by scanning fluorometry. Gag-CFP and Gag-YFP together generated a strong peak at 527 nm upon stimulation of CFP at 433 nm, while CFP and YFP in the absence of Gag generated a peak and a tail curve representing the stimulation of CFP alone (Fig. 2A). In this and each subsequent experiment, the quantity of each YFP and CFP construct was determined by measuring YFP fluorescence to ensure that the acceptor YFP levels were approximately equal in each comparison (Fig. 2A). Deletion of p6 had no effect on Gag-Gag FRET (MACANC) (Fig. 2B). However, a G2A mutation in MA that eliminates the myristoyl acceptor glycine residue completely eliminated Gag-Gag interaction [Myr(−)MACANC] (Fig. 2B). To further test the role of myristoylation in Gag-Gag interactions, the MA domain was replaced with the N-terminal 10 residues from v-*src*. This conferred a heterologous myristoylation signal on the N terminus of the CANC protein. FRET was readily apparent with this construct (Fig. 2C). CANC without the v-*src* sequence failed to generate a FRET signal (Fig. 2C). In order to further establish that myristoylation and not another effect from the v-*src* resi-

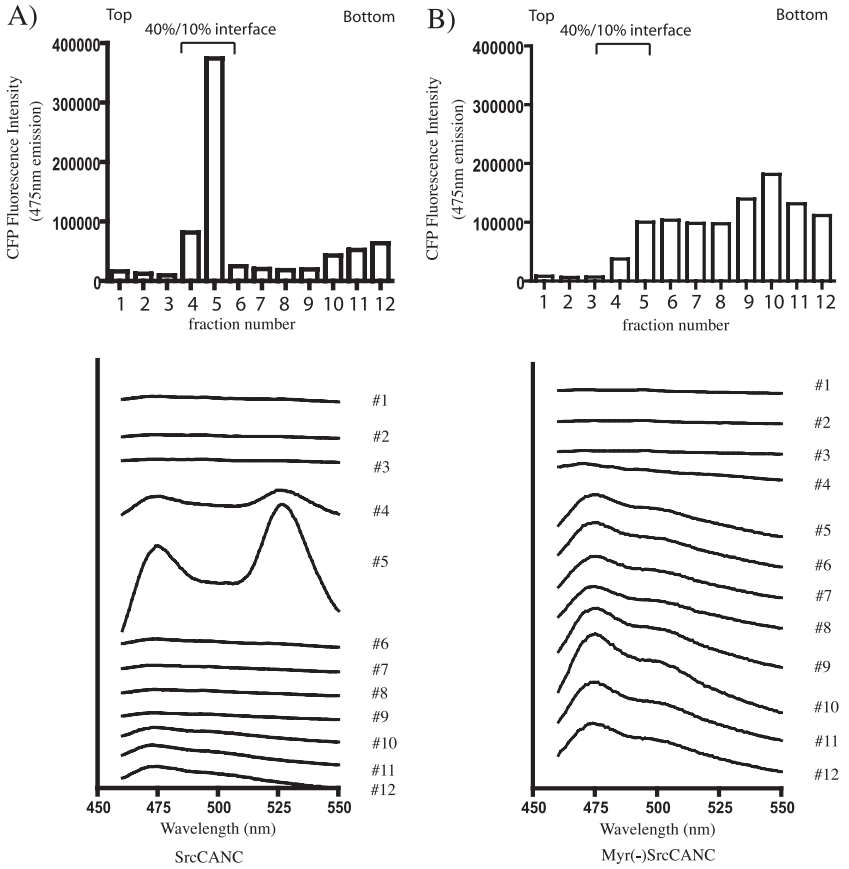

FIG. 3. Membrane flotation centrifugation of SrcCANC (A) and Myr(−)SrcCANC (B). Cell lysates were layered on the bottom of a 50%–40%–10% iodixanol gradient, and equilibrium flotation centrifugation was carried out to separate membranes (40%–10% interface) from cytosol (fractions 6 to 12). Top bars indicate CFP fluorescence as a marker of total Gag protein in the membrane or cytosol. Bottom curves represent emission scans for each individual gradient fraction.

dues accounted for the dramatic difference in the FRET signal, the myristoyl acceptor glycine of the v-*src* sequence in SrcCANC was changed to an alanine residue. This change reproduced the lack of FRET seen with the other nonmyristoylated Gag proteins (Fig. 2C, closed circles). Together, these data establish the importance of myristic acid for Gag-Gag interactions within living cells.

Gag-Gag interactions occur on cellular membranes. The presence of a myristoyl group could potentially enhance Gag-Gag multimerization by enhancing Gag-membrane interactions. We separated cellular membranes from cytosol by flotation centrifugation and examined each fraction of the gradient for CFP fluorescence and for CFP-YFP FRET. SrcCANC (myristoylated) was found predominantly, but not exclusively, in the interface between 10% and 40% iodixanol corresponding to cellular membranes (fractions 4 and 5) (Fig. 3A, top). The corresponding emission scans following excitation at 433 nm revealed that only fractions 4 and 5 had significant FRET (527-nm emission peak) (Fig. 3A, bottom). Nonmyristoylated SrcCANC was predominantly cytosolic, as indicated by the peak signal outside of membrane fractions 4 and 5 (Fig. 3B, bar graph). No FRET signal was observed for Myr(−)SrcCANC in cytosolic or membrane fractions (Fig. 3B, bottom emission scan tracings). These results indicate that Gag-Gag FRET is observed for myristoylated Gag and occurs on cellular membranes.

Role of CA in Gag-Gag interactions. CA-CA interactions clearly play an essential role in Gag-Gag multimerization. While a crystal structure detailing contacts between Gag molecules in the immature particle core is not yet available, there is evidence for the involvement of both CTD-CTD and NTD-NTD interactions prior to maturation (25, 41). We sought to determine if selected amino acid changes in CA would abrogate Gag-Gag interactions measured by FRET in living cells. First, we examined CA with the N-terminal myristoylation signal from v-*src* (SrcCA) (Fig. 4A). Nonmyristoylated CA-CFP and CA-YFP did not produce detectable FRET signal in cells (data not shown). The addition of the N-terminal 10 residues from v-*src* resulted in a very low-level peak that was equivalent to that seen for CFP and YFP fused to the same myristoylation signal (22) (Fig. 4A). CA in this context thus did not seem to contribute to FRET. In contrast, the level of FRET produced by a myristoylated SP1-NC fragment was higher but did not reach that of myristoylated CANC (Fig. 4A). Total levels of CFP and YFP fluorescent signals were measured and were comparable between constructs in each of these comparisons. These data suggested that the FRET signal from CA-CA interactions was very weak in the absence of NC

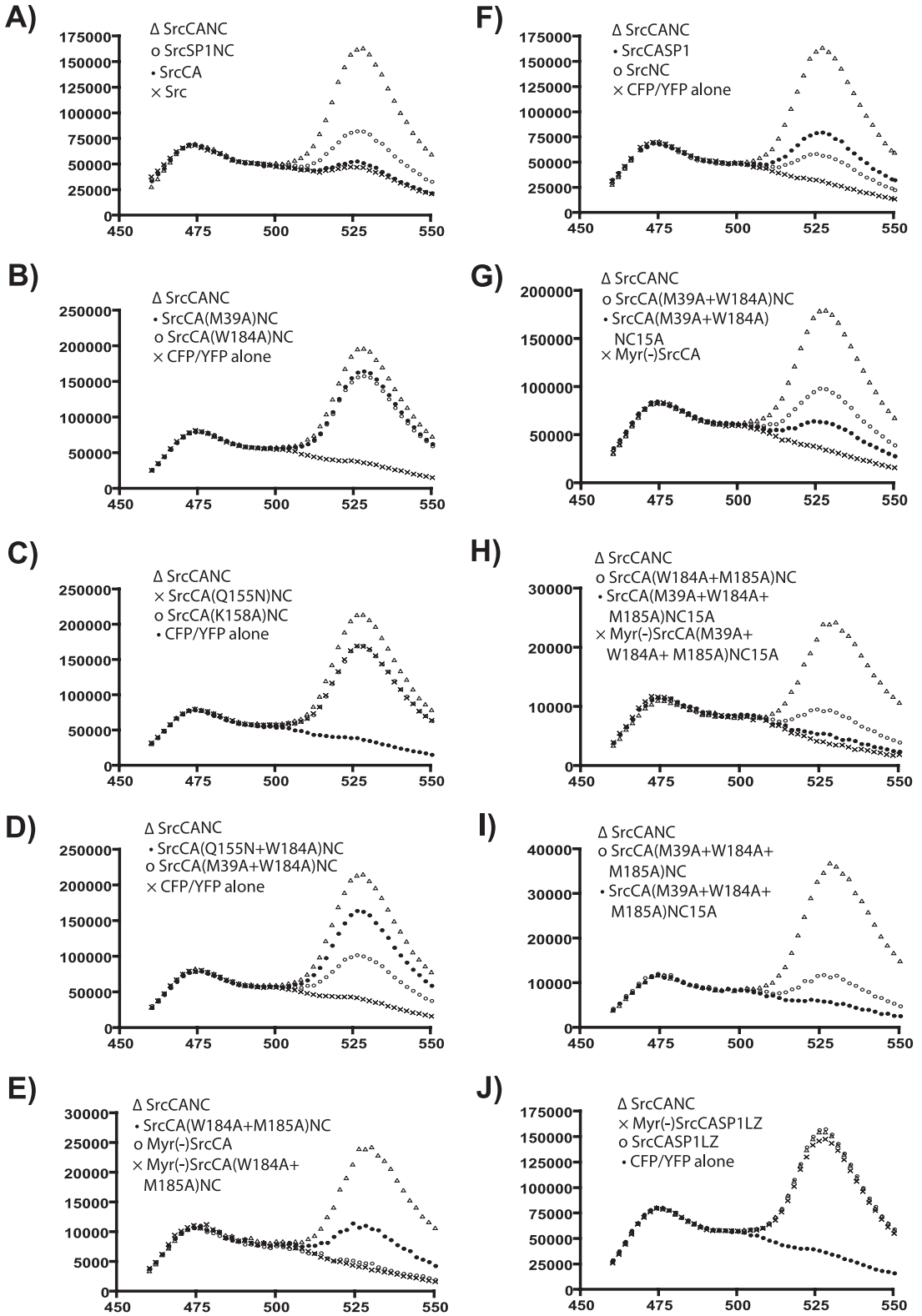

FIG. 4. Emission scan results for panels of Gag-CFP/YFP paired constructs. SrcCANC serves as a positive FRET control in each frame. YFP emission values are not shown in this panel due to space considerations but were of approximately equal intensity for each comparison. A key is included with each panel indicating the specific constructs examined. Details of each comparison in A to J are provided in Results.

and led us to examine the contribution of individual amino acid changes within CA in the context of the larger SrcCANC construct.

We next evaluated four selected mutations that might disrupt Gag-Gag interactions. The selected changes included methionine 39 (M39) in helix 2 of the CA NTD, tryptophan 184 (W184) in the dimer interface of the CA CTD, and glutamine 155 (Q155) and lysine 158 (K158) in the MHR of the CA CTD. The M39 mutation has been shown to disrupt normal particle assembly, suggesting that this change may disrupt CA-CA contacts involved in the immature virion (40). W184 is located in the dimer interface, which appears to be important for CA-CA contacts in both mature and immature virions (41). Q155 is an invariant residue in the MHR; mutation of this residue greatly impairs particle production (29) and was recently predicted to form key hydrogen bonds, stabilizing interactions of the CA CTD modeled on the zinc finger-associated SCAN domain (22). Disruption of K158 reduces particle formation severely (41) and is also predicted to be important for the domain-swapped CA dimer interface predicted by the SCAN motif (22). Thus, we hypothesized that each of these residues could be critical for CA-CA interactions during assembly. Each residue was changed individually to alanine and tested in the context of SrcCANC-CFP and SrcCANC-YFP for interaction as measured by FRET. Indeed, a small decrease in the FRET peak was observed for each of the individual mutations (Fig. 4B and C) compared with SrcCANC. However, none of the changes individually abolished Gag-Gag interactions. We therefore evaluated combinations of the individual alanine mutants. No double combination completely eliminated the Gag-Gag interaction. However, the combination of M39A and W184A (Fig. 4D) or W184A and M185A (Fig. 4E) led to FRET peaks that were comparable to that seen with SrcSP1NC (Fig. 4A). Thus, it seemed unlikely that we could completely eliminate Gag-Gag interactions through targeted mutations in the CA NTD and CA CTD as long as the contributions of myristoylation and of NC were present. Because myristic acid had already been shown to be essential for Gag-Gag FRET, we next examined combinations that included the disruption of basic charges in NC.

Role of NC in Gag-Gag interactions. To verify that NC contributed to Gag-Gag interactions in this assay system, myristoylated NC-CFP and NC-YFP fusion proteins (SrcNC in Fig. 1 and Fig. 4) were expressed and evaluated by scanning fluorometry. SrcNC generated a low but measurable FRET peak (Fig. 4F). NC has been suggested to contribute to Gag-Gag interactions by tethering Gag together on the RNA and facilitating protein-protein interactions contributed by other regions of Gag (4, 8, 36). We tested the role of basic residues in NC in contributing to Gag-Gag interaction by substituting each of the 15 basic residues with alanine (NC15A) and then performing FRET analysis of SrcCANC15A in combination with the previously described CA mutations that diminished but did not eliminate FRET. Expression of NC15A in combination with CA NTD (M39A) and CTD (W184A) mutations further reduced but again failed to completely eliminate FRET (Fig. 4G, closed circles versus open circles). Only upon the introduction of a second change in the CTD dimer interface (M185A) in combination with the W184A and M39A mutations in CA together with NC15A was Gag-Gag interactions completely eliminated (Fig. 4H, closed circles). The contribution of basic charges within NC to Gag-Gag interactions was easily appreciated in the context of the SrcCA(M39A/W184A/M185A) fusion protein, as FRET was detected with a wild-type NC but not in the presence of NC15A (Fig. 4I). These results support a model in which the basic charge within NC can bring Gag molecules together, whereupon CA-CA interactions that depend upon contacts within both the NTD and CTD occur. As described above, these interactions also required myristic acid (Fig. 4).

Forced multimerization using an LZ eliminates the requirement for myristic acid in Gag-Gag multimerization. The finding that myristic acid was required for Gag-Gag interactions in live cells was surprising. It has been known for some time that LZ domains can substitute for the assembly function of NC (43). We next asked if the replacement of NC with an LZ altered the requirement for myristic acid. We replaced NC in both myristoylated and nonmyristoylated SrcCASP1 constructs with the LZ from the yeast transcription factor GCN4 and evaluated the ability of these artificial Gag constructs to interact, as measured by FRET. Remarkably, both myristoylated and nonmyristoylated LZ constructs exhibited strong FRET peaks equal to that of SrcCANC (Fig. 4J). Thus, the replacement of NC with an LZ eliminated the need for myristoylation in bringing Gag molecules together in cells.

In the absence of the LZ domain, we were unable to detect FRET outside of membrane fractions for any of the Gag-CFP/Gag-YFP pairs (data discussed above). We then asked if the multimerization conferred by the LZ eliminated the exclusive appearance of multimers on membranes. SrcCASP1LZ was present in both membrane and cytosolic fractions following membrane flotation (Fig. 5A, top). CFP/YFP FRET was observed only in the membrane fractions (fractions 4 and 5 from the 40%–10% interface) (Fig. 5A, bottom curves). Myr(−)SrcCASP1LZ was predominantly cytosolic (Fig. 5B, top). CFP/YFP FRET was distributed throughout the gradient, with some in the membrane fraction (fractions 4 and 5) and additional signal in fractions 6 to 8. The 527-nm YFP peak was not easily appreciated in the bottom fractions (fractions 9 to 12) and may have been hidden by the tail of the CFP emission curve (Fig. 5B, bottom). These results suggest that Gag-Gag interactions can occur in the absence of cellular membranes when NC is replaced with an LZ domain, while in the case of the myristoylated LZ construct, Gag-Gag interactions occur on cellular membranes. Alternatively, the appearance of FRET in both membrane and cytosolic fractions in Fig. 5B may reflect weak membrane interactions that were largely dissociated during gradient fractionation.

Rescue of myristoylation-deficient Gag into Gag-Gag complexes by myristoylated Gag. The data outlined above indicate that Gag-Gag interactions occur on cellular membranes and that myristoylation is required for multimerization except when a strong protein-protein interaction domain such as an LZ is introduced. Another measure of Gag-Gag interactions can be derived from the rescue of deficient Gag molecules into membrane fractions or particles. We modified this assay to ask if the nonmyristoylated Gag-YFP could be recruited into multimers by myristoylated Gag-CFP. Indeed, Myr(−)SrcCANC was efficiently rescued into complexes by myristoylated SrcCANC (Fig. 6A). Rescue was reduced but not eliminated for

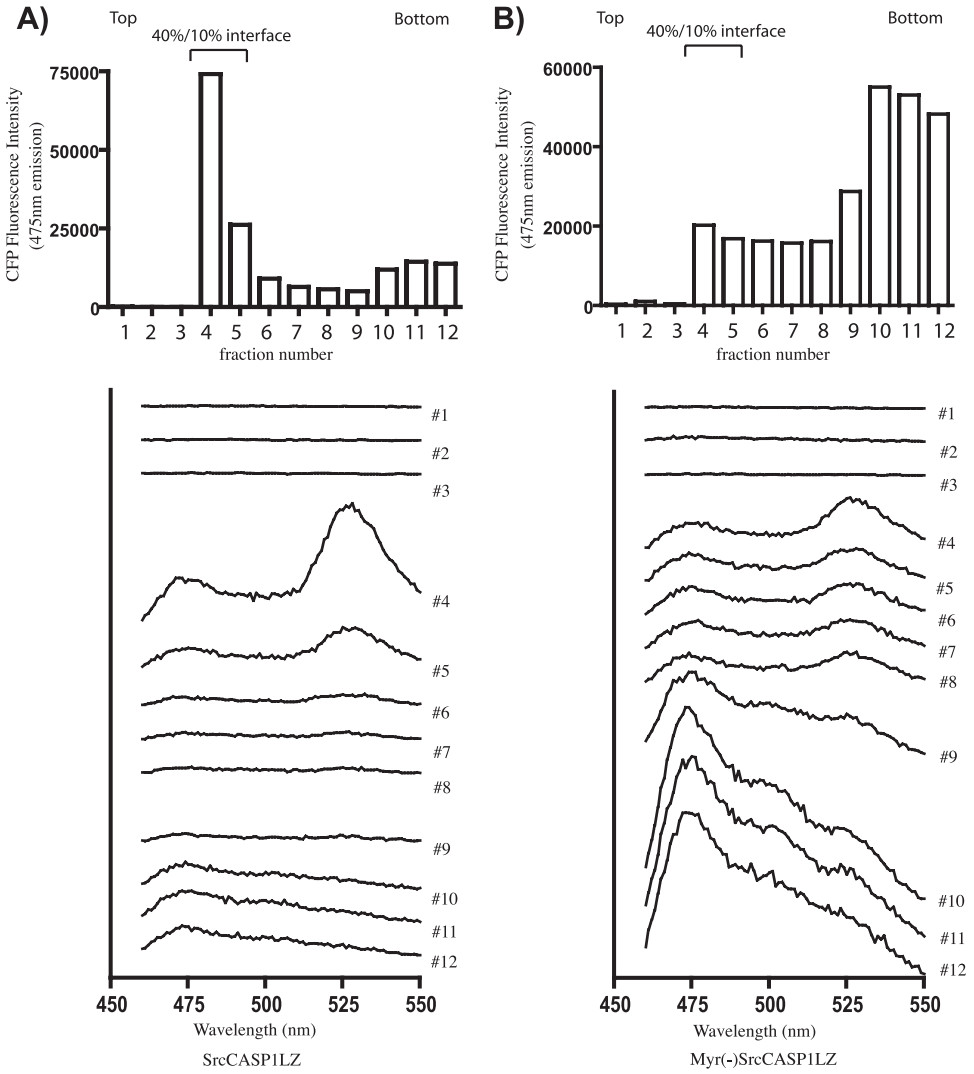

FIG. 5. Membrane flotation centrifugation of SrcCASP1LZ (A) and Myr(−)SrcCASP1LZ (B). Cell lysates were layered onto the bottom of a 50%–40%–10% iodixanol gradient, and equilibrium flotation centrifugation was carried out to separate membranes (40%–10% interface) from cytosol (fractions 6 to 12). Top bars indicate CFP fluorescence as a marker of total Gag protein in the membrane or cytosol. Bottom curves represent emission scans for each individual gradient fraction following stimulation with 433 nm light.

constructs bearing mutations in the CA CTD dimer interface (W184A and M185A) or combinations of NTD and CTD mutations (M39A, W184A, and M185A). Remarkably, only the combination of M39A, W184A, and NC15A with or without M185A eliminated all rescue of the nonmyristoylated Gag protein into complexes (Fig. 6A). These data are consistent with the data shown in Fig. 4I, in which this combination of CA and NC substitutions eliminated Gag-CFP/Gag-YFP FRET in the context of myristoylated Gag. The M39A, W184A, W185A, and NC15A substitutions therefore appear to eliminate Gag-Gag interactions and prevent rescue into Gag multimers by myristoylated SrcCANC.

Subcellular localization of Gag-CFP/Gag-YFP proteins. The cellular distribution of the major fusion protein constructs utilized in this study was examined by confocal microscopy in order to correlate distribution with the conclusions reached regarding myristoylation and membrane interaction. MACANC at late times posttransfection was predominantly found at the plasma membrane (Fig. 7A), while its nonmyristoylated counterpart was diffusely cytosolic (Fig. 7B). SrcCANC had a plasma membrane distribution very similar to that of MACANC (Fig. 7C); Myr(−)SrcCANC was diffusely cytosolic but also collected in perinuclear regions (Fig. 7D). It is interesting that despite these large, bright, perinuclear collections, this construct was not capable of forming Gag-Gag multimers. The myristoylated LZ construct (SrcCASP1LZ) appeared to be identical to MACANC or SrcCANC in its plasma membrane distribution (Fig. 7E). Remarkably, the nonmyristoylated SrcCASP1LZ was diffusely cytosolic, with no discernible plasma membrane fluorescence. Finally, the apparent monomer SrcCA(M39A/W184A/M185A)NC15A demonstrated an unusual reticular appearance, with signal at the plasma membrane and on intracellular membranes but lacking bright puncta at any point in the cell (Fig. 7G). Its nonmyristoylated

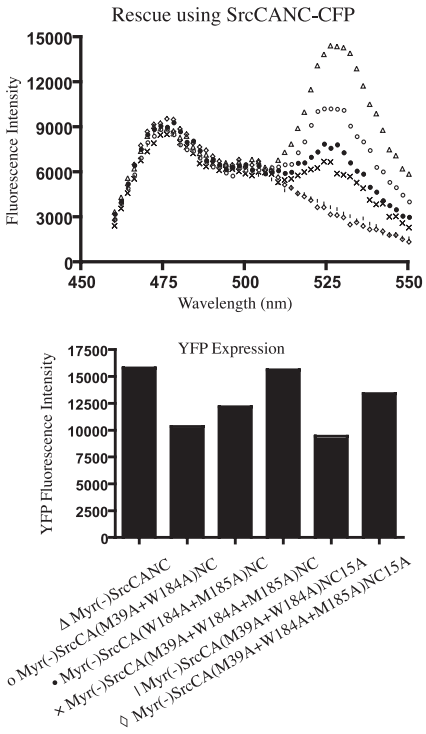

FIG. 6. FRET rescue experiments. SrcCANC-CFP was cotransfected with each of the indicated nonmyristoylated constructs fused to YFP, and emission scanning was performed to examine FRET. The symbol key is present below YFP intensity bars. All constructs demonstrate FRET as rescued by the myristoylated construct, except for Myr(−)SrcCA(M39A/W184A)NC15A and Myr(−)SrcCA(M39A/W184A/M185A)NC15A, which are represented as vertical lines and diamonds, respectively.

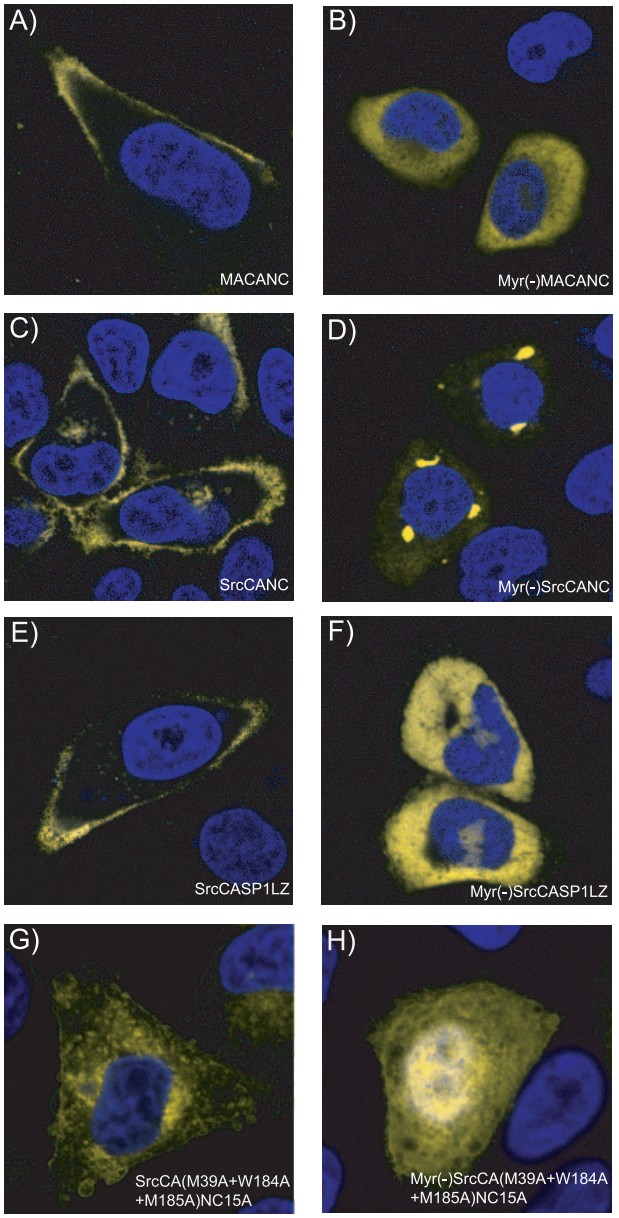

FIG. 7. Laser scanning confocal fluorescence microscopy of key Gag fusion proteins. Shown are HeLa cells transfected with the YFP fusion partner of paired constructs examined using a Zeiss LSM 510 confocal microscope. Myristoylated constructs are shown on the left, and the nonmyristoylated counterparts are on the right. DAPI (4′,6′-diamidino-2-phenylindole) counterstain was used to provide nuclear stain. (A) MACANC; (B) Myr(−)MACANC; (C) SrcCANC; (D) Myr(−)SrcCANC; (E) SrcCASP1LZ; (F) Myr(−)SrcCASP1LZ; (G) ScrCA(M39A/W184A/M185A)NC15A; (H) Myr(−)ScrCA(M39A/W184A/M185A)NC15A.

counterpart was also somewhat reticular but was more diffusely cytosolic and included prominent nuclear localization. These data generally support the findings from fractionation studies that multimerization-competent Gag constructs are present on cellular membranes (Fig. 7, left), while nonmyristoylated, multimerization-incompetent constructs are predominantly cytosolic (right). The two important exceptions to this include Myr(−)SrcCASP1LZ, which is cytosolic but multimerization competent (Fig. 7F), and SrcCA(M39A/W184A/M185A)NC15A, which is membrane associated but fails to multimerize (Fig. 7G).

DISCUSSION

Contacts between CA molecules in the mature core of virions have been defined through the use of X-ray crystallography of purified proteins combined with electron cryomicroscopic reconstruction of CA cylinders and virions (15, 16, 26). The dimer interface of the CA CTD contains key residues (W184 and M185) that are essential to particle infectivity, conical core formation, and particle production, suggesting that contacts in this site are present in the immature Gag protein shell and the mature core. Additional CA-CA contacts within the immature Gag shell are less well defined, but mutagenesis studies have clearly established the importance of both the NTD and CTD in immature particle formation (40, 41). Alterations of CA residues outside of obvious contact sites can also disrupt particle formation, including residues within the highly conserved MHR (29), and the C-terminal 11 residues of CA (27). The adjacent 14-residue SP1 is also somewhat sensitive to mutations, one of which potently disrupts Gag-Gag multimerization and particle production (21), although some mutations in this region are tolerated (1). The majority of evidence in the literature suggests that CA-CA contacts, perhaps in conjunction with residues in SP1, are required for Gag-Gag multimerization and subsequent assembly.

It is less certain how NC contributes to Gag-Gag interactions. In vitro particle formation studies strongly suggest a tethering model in which NC binding to nucleic acid brings Gag molecules together and facilitates multimerization (8, 9). An attractive model has been proposed based upon the length of the oligonucleotide that promoted efficient assembly in vitro. According to this model, nucleic acid binding promotes the dimerization of Gag, and the resulting dimer then becomes an essential intermediate contributing to higher-order multimerization (28). This interpretation is consistent with the fact that dimerizing LZs can functionally replace NC in its role in particle formation (23, 43). NC is essential for the formation of particles of normal density and for the formation of detergent-resistant Gag complexes in cells (13, 35). The proper formation of an intermediate, potentially a Gag dimer, through NC-RNA interactions could explain these findings.

In this study, we found that the myristoylation of Gag is essential for Gag-Gag multimerization in cells. This result was unexpected, because in vitro models of particle assembly do not require myristoylated Gag protein. The most straightforward explanation for this observation is that membrane interactions facilitated by myristic acid act to enhance the direct protein-protein interactions elsewhere in the molecule, most notably those within CA or CA and SP1. This finding implies that retroviral Gag proteins are stimulated to multimerize through "tethers" at or near both the N terminus (myristic acid or myristic acid plus basic residues interacting with cellular membranes) and the C terminus (NC interacting with nucleic acid). This model would help to explain why most retroviral Gag molecules normally do not form particles free in the cytoplasm, a dead-end route that would be disadvantageous to the virus. It is interesting that the betaretrovirus Mason-Pfizer monkey virus, which does assemble immature capsids within the cytoplasm, contains an internal scaffolding domain within its p12 segment, which lies N terminal to CA (34). We propose that membrane interactions in which myristic acid is required can perform a similar scaffolding or concentrating role for HIV Gag as the internal scaffolding domain does for Mason-Pfizer monkey virus.

Some extremely high-level expression systems allow intracellular particles to form when nonmyristoylated Gag protein is produced. Most notable is the baculovirus expression system, where assembly of immature core-like structures in the cytoplasm of insect cells as well as dense nuclear aggregates have been observed (10, 18). In the present study, however, we used a high-level mammalian expression system and observed no Gag-Gag multimerization in the absence of myristoylation. It is possible that myristic acid serves to concentrate Gag molecules on cellular membranes, and under most expression conditions, this concentration effect is required to trigger multimerization. Insect cell expression may be sufficiently high that this concentrating effect of myristic acid is not required.

Myristoylated Gag proteins in the present study were able to multimerize less efficiently when CA mutations that were predicted to disrupt functional contacts in the CA NTD or CA CTD were introduced. Combinations of mutations further reduced but did not eliminate Gag-Gag interactions when NC was not altered. Elimination of all basic residues within NC (NC15A), in combination with disruption of the NTD and CTD, resulted in a monomeric, myristoylated Gag protein. A nonmyristoylated version of this "monomer Gag" construct could not be rescued into Gag-Gag interactions by myristoylated Gag. It should be noted that a myristoylated "mini-Gag" construct lacking the CA NTD can assemble retrovirus-like particles, pointing out that NTD-NTD contacts are not absolutely required for Gag-Gag multimerization, at least in this context (2, 3). However, the FRET study reported here suggests that NTD-NTD interactions (specifically, the M39 residue in CA helix II) do contribute to Gag-Gag interactions in the context of immature core formation. This is supported by mutagenesis data (41) and by hydrogen-deuterium exchange experiments (25) in which NTD-NTD interactions were noted to be present in both mature and immature viral particles. Taken together, these data suggest a model in which there are three essential requirements for Gag-Gag multimerization: basic residues within NC, membrane binding facilitated by myristic acid, and direct protein-protein interactions mediated by CA. The requirement for basic residues in NC likely reflects a requirement for nucleic acid binding.

Substitution of a dimerizing LZ for NC removed the requirement for myristoylation to drive Gag-Gag multimerization in this study. The finding that an LZ can substitute for NC is not novel, but here, this substitution allowed us to establish that the methods used for detecting Gag-Gag interactions by FRET do not prevent the detection of a cytosolic FRET signal if Gag molecules are forced together in the absence of a membrane anchor. We suggest that the LZ is able to substitute for the influence of both myristic acid-membrane interactions and NC-nucleic acid interactions in initiating and securing Gag-Gag interactions. The strong thermal stability of the LZ dimer is likely superior to that of CA-CA contacts within Gag alone, which are normally assisted by NC/RNA and myristoylated MA/membrane anchors.

There are limitations to this study and areas that require further work. The identification of all key residues within CA or SP1 that are required for multimerization was not the focus of the study. We recognize that a number of additional mutations may have disrupted direct protein-protein interactions in CA or SP1. Complete mapping of these residues is an important goal that we did not attempt to address here. Because the combination of one NTD and two CTD changes was sufficient to disrupt the contribution of CA to Gag-Gag FRET, we did not comprehensively survey other mutations. Our study also did not fully address the role of MA in Gag-Gag multimerization. The highly basic MA protein has been reported to bind RNA and potentially contribute to Gag-Gag interactions (7). Finally, although we could detect FRET initiated by Gag-CFP/YFP molecules with dimerizing LZs, we have not established that the fluorometric assay chosen can detect one or a few dimers of Gag. The limitations of detection of this assay are under study at present using LZ/CFP-YFP dimers in vitro.

It will be extremely interesting to further characterize the myristoylated M39A/W184/M185A/NC15A Gag molecule. This molecule is a monomer by FRET and cannot be rescued into particles by wild-type Gag (data not shown). Monomeric Gag may be useful for analyzing early trafficking steps in the assembly pathway and for dissecting interactions with cellular proteins that may occur exclusively with Gag oligomers or assembly intermediates.

In summary, we propose a three-component model for Gag-Gag multimerization. According to this model, the tethering of Gag by nucleic acid and the interaction of the myristoylated N terminus of Gag with cellular membranes act in concert to facilitate direct protein-protein contacts within CA or CA and SP1. The requirement for multimerization on cellular membranes may represent a means by which many retroviruses prevent the nonproductive formation of immature capsids in the cytoplasm of infected cells.

ACKNOWLEDGMENTS

This work was supported primarily by NIH R01 AI67101 and partially by NIH R01 AI40338.

We acknowledge intellectual and infrastructure support from the Emory Center for AIDS Research. We thank Gary Nabel (VRC, NIH) for the gift of the pVRC3900 plasmid from which the original codon-optimized *gag* sequence was derived, Chen Liang (McGill AIDS Center, Montreal, Canada) for the GCN4 LZ cDNA, and the Winship Cancer Institute Cell Imaging and Microscopy Core at Emory University for assistance with confocal microscopy. We thank David Piston (Vanderbilt University, Nashville, TN) for the cerulean cDNA and Atsushi Miyawaki (Brain Science Institute, Saitama, Japan) for the Venus cDNA.

REFERENCES

1. **Accola, M. A., S. Hoglund, and H. G. Gottlinger.** 1998. A putative alpha-helical structure which overlaps the capsid-p2 boundary in the human immunodeficiency virus type 1 Gag precursor is crucial for viral particle assembly. J. Virol. **72:**2072–2078.
2. **Accola, M. A., B. Strack, and H. G. Gottlinger.** 2000. Efficient particle production by minimal Gag constructs which retain the carboxy-terminal domain of human immunodeficiency virus type 1 capsid-p2 and a late assembly domain. J. Virol. **74:**5395–5402.
3. **Borsetti, A., A. Ohagen, and H. G. Gottlinger.** 1998. The C-terminal half of the human immunodeficiency virus type 1 Gag precursor is sufficient for efficient particle assembly. J. Virol. **72:**9313–9317.
4. **Bowzard, J. B., R. P. Bennett, N. K. Krishna, S. M. Ernst, A. Rein, and J. W. Wills.** 1998. Importance of basic residues in the nucleocapsid sequence for retrovirus Gag assembly and complementation rescue. J. Virol. **72:**9034–9044.
5. **Briggs, J. A., T. Wilk, R. Welker, H. G. Krausslich, and S. D. Fuller.** 2003. Structural organization of authentic, mature HIV-1 virions and cores. EMBO J. **22:**1707–1715.
6. **Bryant, M., and L. Ratner.** 1990. Myristoylation-dependent replication and assembly of human immunodeficiency virus 1. Proc. Natl. Acad. Sci. USA **87:**523–527.
7. **Burniston, M. T., A. Cimarelli, J. Colgan, S. P. Curtis, and J. Luban.** 1999. Human immunodeficiency virus type 1 Gag polyprotein multimerization requires the nucleocapsid domain and RNA and is promoted by the capsid-dimer interface and the basic region of matrix protein. J. Virol. **73:**8527–8540.
8. **Campbell, S., and A. Rein.** 1999. In vitro assembly properties of human immunodeficiency virus type 1 Gag protein lacking the p6 domain. J. Virol. **73:**2270–2279.
9. **Campbell, S., and V. M. Vogt.** 1995. Self-assembly in vitro of purified CA-NC proteins from Rous sarcoma virus and human immunodeficiency virus type 1. J. Virol. **69:**6487–6497.
10. **Chazal, N., C. Carriere, B. Gay, and P. Boulanger.** 1994. Phenotypic characterization of insertion mutants of the human immunodeficiency virus type 1 Gag precursor expressed in recombinant baculovirus-infected cells. J. Virol. **68:**111–122.
11. **Dalton, A. K., P. S. Murray, D. Murray, and V. M. Vogt.** 2005. Biochemical characterization of Rous sarcoma virus MA protein interaction with membranes. J. Virol. **79:**6227–6238.
12. **Derdowski, A., L. Ding, and P. Spearman.** 2004. A novel fluorescence resonance energy transfer assay demonstrates that the human immunodeficiency virus type 1 $Pr55^{Gag}$ I domain mediates Gag-Gag interactions. J. Virol. **78:**1230–1242.
13. **Ding, L., A. Derdowski, J. J. Wang, and P. Spearman.** 2003. Independent segregation of human immunodeficiency virus type 1 Gag protein complexes and lipid rafts. J. Virol. **77:**1916–1926.
14. **Franke, E. K., H. E. Yuan, K. L. Bossolt, S. P. Goff, and J. Luban.** 1994. Specificity and sequence requirements for interactions between various retroviral Gag proteins. J. Virol. **68:**5300–5305.
15. **Gamble, T. R., S. Yoo, F. F. Vajdos, U. K. von Schwedler, D. K. Worthylake, H. Wang, J. P. McCutcheon, W. I. Sundquist, and C. P. Hill.** 1997. Structure of the carboxyl-terminal dimerization domain of the HIV-1 capsid protein. Science **278:**849–853.
16. **Ganser, B. K., S. Li, V. Y. Klishko, J. T. Finch, and W. I. Sundquist.** 1999. Assembly and analysis of conical models for the HIV-1 core. Science **283:**80–83.
17. **Ganser-Pornillos, B. K., U. K. von Schwedler, K. M. Stray, C. Aiken, and W. I. Sundquist.** 2004. Assembly properties of the human immunodeficiency virus type 1 CA protein. J. Virol. **78:**2545–2552.
18. **Gheysen, D., E. Jacobs, F. de Foresta, C. Thiriart, M. Francotte, D. Thines, and M. De Wilde.** 1989. Assembly and release of HIV-1 precursor Pr55gag virus-like particles from recombinant baculovirus-infected insect cells. Cell **59:**103–112.
19. **Gottlinger, H. G., J. G. Sodroski, and W. A. Haseltine.** 1989. Role of capsid precursor processing and myristoylation in morphogenesis and infectivity of human immunodeficiency virus type 1. Proc. Natl. Acad. Sci. USA **86:**5781–5785.
20. **Guo, X., and C. Liang.** 2005. Opposing effects of the M368A point mutation and deletion of the SP1 region on membrane binding of human immunodeficiency virus type 1 Gag. Virology **335:**232–241.
21. **Guo, X., A. Roldan, J. Hu, M. A. Wainberg, and C. Liang.** 2005. Mutation of the SP1 sequence impairs both multimerization and membrane-binding activities of human immunodeficiency virus type 1 Gag. J. Virol. **79:**1803–1812.
22. **Ivanov, D., J. R. Stone, J. L. Maki, T. Collins, and G. Wagner.** 2005. Mammalian SCAN domain dimer is a domain-swapped homolog of the HIV capsid C-terminal domain. Mol. Cell **17:**137–143.
23. **Johnson, M. C., H. M. Scobie, Y. M. Ma, and V. M. Vogt.** 2002. Nucleic acid-independent retrovirus assembly can be driven by dimerization. J. Virol. **76:**11177–11185.
24. **Kelly, B. N., B. R. Howard, H. Wang, H. Robinson, W. I. Sundquist, and C. P. Hill.** 2006. Implications for viral capsid assembly from crystal structures of HIV-1 Gag(1–278) and CA(N)(133–278). Biochemistry **45:**11257–11266.
25. **Lanman, J., T. T. Lam, M. R. Emmett, A. G. Marshall, M. Sakalian, and P. E. Prevelige, Jr.** 2004. Key interactions in HIV-1 maturation identified by hydrogen-deuterium exchange. Nat. Struct. Mol. Biol. **11:**676–677.
26. **Li, S., C. P. Hill, W. I. Sundquist, and J. T. Finch.** 2000. Image reconstructions of helical assemblies of the HIV-1 CA protein. Nature **407:**409–413.
27. **Liang, C., J. Hu, J. B. Whitney, L. Kleiman, and M. A. Wainberg.** 2003. A structurally disordered region at the C terminus of capsid plays essential roles in multimerization and membrane binding of the Gag protein of human immunodeficiency virus type 1. J. Virol. **77:**1772–1783.
28. **Ma, Y. M., and V. M. Vogt.** 2002. Rous sarcoma virus Gag protein-oligonucleotide interaction suggests a critical role for protein dimer formation in assembly. J. Virol. **76:**5452–5462.
29. **Mammano, F., A. Ohagen, S. Hoglund, and H. G. Gottlinger.** 1994. Role of the major homology region of human immunodeficiency virus type 1 in virion morphogenesis. J. Virol. **68:**4927–4936.
30. **Nagai, T., K. Ibata, E. S. Park, M. Kubota, K. Mikoshiba, and A. Miyawaki.** 2002. A variant of yellow fluorescent protein with fast and efficient maturation for cell-biological applications. Nat. Biotechnol. **20:**87–90.
31. **Paillart, J.-C., and H. G. Göttlinger.** 1999. Opposing effects of human immunodeficiency virus type 1 matrix mutations support a myristyl switch model of Gag membrane targeting. J. Virol. **73:**2604–2612.
32. **Rizzo, M. A., G. H. Springer, B. Granada, and D. W. Piston.** 2004. An improved cyan fluorescent protein variant useful for FRET. Nat. Biotechnol. **22:**445–449.
33. **Saad, J. S., J. Miller, J. Tai, A. Kim, R. H. Ghanam, and M. F. Summers.** 2006. Structural basis for targeting HIV-1 Gag proteins to the plasma membrane for virus assembly. Proc. Natl. Acad. Sci. USA **103:**11364–11369.
34. **Sakalian, M., S. S. Dittmer, A. D. Gandy, N. D. Rapp, A. Zabransky, and E. Hunter.** 2002. The Mason-Pfizer monkey virus internal scaffold domain enables in vitro assembly of human immunodeficiency virus type 1 Gag. J. Virol. **76:**10811–10820.
35. **Sandefur, S., R. M. Smith, V. Varthakavi, and P. Spearman.** 2000. Mapping and characterization of the N-terminal I domain of human immunodeficiency virus type 1 $Pr55^{Gag}$. J. Virol. **74:**7238–7249.
36. **Sandefur, S., V. Varthakavi, and P. Spearman.** 1998. The I domain is required for efficient plasma membrane binding of human immunodeficiency virus type 1 $Pr55^{Gag}$. J. Virol. **72:**2723–2732.
37. **Spearman, P., R. Horton, L. Ratner, and I. Kuli-Zade.** 1997. Membrane binding of human immunodeficiency virus type 1 matrix protein in vivo supports a conformational myristyl switch mechanism. J. Virol. **71:**6582–6592.
38. **Spearman, P., J. J. Wang, N. Vander Heyden, and L. Ratner.** 1994. Identification of human immunodeficiency virus type 1 Gag protein domains essential to membrane binding and particle assembly. J. Virol. **68:**3232–3242.
39. **Tang, C., E. Loeliger, P. Luncsford, I. Kinde, D. Beckett, and M. F. Summers.** 2004. Entropic switch regulates myristate exposure in the HIV-1 matrix protein. Proc. Natl. Acad. Sci. USA **101:**517–522.
40. **von Schwedler, U. K., T. L. Stemmler, V. Y. Klishko, S. Li, K. H. Albertine, D. R. Davis, and W. I. Sundquist.** 1998. Proteolytic refolding of the HIV-1

capsid protein amino-terminus facilitates viral core assembly. EMBO J. **17:**1555–1568.

41. **von Schwedler, U. K., K. M. Stray, J. E. Garrus, and W. I. Sundquist.** 2003. Functional surfaces of the human immunodeficiency virus type 1 capsid protein. J. Virol. **77:**5439–5450.
42. **Worthylake, D. K., H. Wang, S. Yoo, W. I. Sundquist, and C. P. Hill.** 1999. Structures of the HIV-1 capsid protein dimerization domain at 2.6 A resolution. Acta Crystallogr. D Biol. Crystallogr. **55:**85–92.
43. **Zhang, Y., H. Qian, Z. Love, and E. Barklis.** 1998. Analysis of the assembly function of the human immunodeficiency virus type 1 Gag protein nucleocapsid domain. J. Virol. **72:**1782–1789.
44. **Zhou, W., L. J. Parent, J. W. Wills, and M. D. Resh.** 1994. Identification of a membrane-binding domain within the amino-terminal region of human immunodeficiency virus type 1 Gag protein which interacts with acidic phospholipids. J. Virol. **68:**2556–2569.
45. **Zhou, W., and M. D. Resh.** 1996. Differential membrane binding of the human immunodeficiency virus type 1 matrix protein. J. Virol. **70:**8540–8548.